Ecological Applications, 26(1), 2016, pp. 55–66

Hemiparasite–host plant interactions in a fragmented landscape assessed via imaging spectroscopy and LiDAR

Jomar M. Barbosa[1,2,4] Esther Sebastián-González[2,3] Gregory P. Asner[1] David E. Knapp[1] Christopher Anderson[1] Roberta E. Martin[1] and Rodolfo Dirzo[2]

[1]*Department of Global Ecology, Carnegie Institution for Science, Stanford, California 94305 USA*
[2]*Department of Biology, Stanford University, Stanford, California 94305 USA*
[3]*Department of Ecology, University of São Paulo, São Paulo 05508-090 Brazil*

Abstract. Species interactions are susceptible to anthropogenic changes in ecosystems, but this has been poorly investigated in a spatially explicit manner in the case of plant parasitism, such as the omnipresent hemiparasitic mistletoe–host plant interactions. Analyzing such interactions at a large spatial scale may advance our understanding of parasitism patterns over complex landscapes. Combining high-resolution airborne imaging spectroscopy and LiDAR, we studied hemiparasite incidence within and among tree host stands to examine the prevalence and spatial distribution of hemiparasite load in ecosystems. Specifically, we aimed to assess: (1) detection accuracy of mistletoes on their oak hosts; (2) hemiparasitism prevalence within host tree canopies depending on tree height, and (3) spatial variation in hemiparasitism across fragmented woodlands, in a low-diversity mediterranean oak woodland in California, USA. We identified mistletoe infestations with 55–96% accuracy, and detected significant differences in remote-sensed spectra between oak trees with and without mistletoe infestation. We also found that host canopy height had little influence on infestation degree, whereas landscape-level variation showed consistent, nonrandom patterns: isolated host trees had twice the infestation load than did trees located at the core of forest fragments. Overall, we found that canopy exposure (i.e., lower canopy density or proximity to forest edge) is more important than canopy height for mistletoe infestation, and that by changing landscape structure, parasitic prevalence increased with woodland fragmentation. We conclude that reducing fragmentation in oak woodlands will minimize anthropogenic impact on mistletoe infestation at the landscape level. We argue that advanced remote sensing technology can provide baselines to quantitatively analyze and monitor parasite–host trajectories in light of global environmental change, and that this is a promising approach to be further tested in other temperate and tropical forests.

Key words: detection of host–parasite interactions; forest fragmentation; Jasper Ridge Biological Preserve; mistletoes; oak forest; Carnegie Airborne Observatory

Introduction

Land use change is one of the most important and widespread challenges for biological conservation worldwide (Sala et al. 2000, Echeverria et al. 2006, Underwood et al. 2009, Bennett and Saunders 2010, Costa et al. 2014). As a consequence of the current anthropogenic increase in habitat loss, many animal and plant communities are undergoing changes in abundance and richness (Sala et al. 2000, Fahrig 2003). When a habitat is fragmented, the proportion of edge substantially increases, favoring those species adapted to the new conditions, often to the detriment of species requiring interior habitat environments (Debinski and Holt 2000, Terborgh et al. 2001, Laurance et al. 2011). Moreover, species alter their dispersion patterns as vegetation is redistributed in the fragmented landscape (Fletcher et al. 2007).

Many studies have described the effects of habitat fragmentation on species abundance and diversity in tropical forests (Joly et al. 2014, Villard and Metzger 2014) and in temperate forests (Willson et al. 1994, Cooper and Walters 2002, Underwood et al. 2009). Other studies examined the consequences of fragmentation on species interactions, particularly mutualisms

Manuscript received 17 December 2014; revised 7 April 2015; accepted 10 April 2015. Corresponding Editor: D. S. Schimel.
[4]E-mail: jomarmbarbosa@gmail.com

(e.g., Rodríguez-Cabal et al. 2007, Cagnolo et al. 2008) and a few on antagonistic interactions such as herbivory (Fáveri et al. 2008, Ruiz-Guerra et al. 2010). In contrast, the effects of fragmentation on plant hemiparasitism on host trees (phorophytes) have been very poorly investigated in a spatially explicit manner, despite the fact this is an omnipresent interaction worldwide, as is the case of mistletoes and their phorophytes (Watson 2001), and despite the fact such plant–hemiparasite interactions are also known or expected to be aggravated by human-mediated changes in ecosystems (Rodríguez-Cabal et al. 2007, MacRaild et al. 2010). For example, as many hemiparasitic plants are dispersed by birds (Watson 2001), habitat loss that affects bird foraging behavior may change the distribution and level of phorophyte infestation. Changes in hemiparasitic plant abundance may affect host physiology and fitness at the individual and population levels (Hollinger 1983, Meinzer et al. 2004), especially where rates of hemiparasitic infestation are high. Therefore, changes in landscape structure may have strong cascading effects on the community of phorophytes and hemiparasites (Magrach et al. 2013, 2014). Identifying hemiparasite outbreaks at broad ecological scales, as well as understanding how landscape structure determines the hemiparasite prevalence and load on their host plants, are central to the ecology and management of areas where parasitic and hemiparasitic plants are present.

Some aspects of the effect of fragmentation on the interaction between mistletoes and their phorophytes has been previously explored by a few studies. MacRaild et al. (2010) found that habitat fragmentation initially enhances mistletoe occurrence while López de Buen et al. (2002) found that mistletoes have higher abundance in forest edges than in core areas of forest fragments. These studies assessed mistletoe prevalence and its variation in space; however, they did not analyze mistletoe prevalence weighted by total host availability. At a larger scale, information about mistletoe prevalence in the host population and how forest structure mediates parasite–host interaction is limited because of the difficulty of mapping infestation prevalence on landscapes.

On the other hand, remote sensing has been used for the detection and mapping of the impacts of insect infestation processes in temperate forests, such as for mountain pine beetles (Wulder et al. 2006), providing useful spatial mapping information that could inform more detailed studies of host–pest interactions. New technologies, such as high-resolution imaging spectroscopy and airborne Light Detection and Ranging (LiDAR), expand the ways to map species composition and vegetation structure, respectively (Baldeck et al. 2014). Recent imaging spectroscopy advances in the second Carnegie Airborne Observatory (CAO) have improved detection of species (Asner et al. 2012) and therefore we explored if, combined, the two technologies may help to understanding spatially explicit changes in hemiparasite–phorophyte interactions mediated by fragmentation of natural habitat.

Our study is focused on four plant species: the hemiparasitic *Phoradendron leucarpum* (mistletoe) and its oak tree phorophytes (*Quercus lobata*, *Q. douglasii*, *Q. kellogii*) in the study area. The genus *Quercus* has a worldwide distribution, with recognized ecological and economical importance. Mistletoes are well-known hemiparasitic species that occur throughout the world (Watson 2001). They are keystone species in woodlands and forests because they provide high-quality food and nesting or roosting sites for many animals (Watson 2001, 2002, Cooney and Watson 2005, Cooney et al. 2006). However, from the phorophyte's perspective, mistletoes can be highly detrimental. They decrease the fitness of their phorophytes via their negative effects on vegetative and reproductive performance or survival at individual level (Reid et al. 1994, Norton and Carpenter 1998, Mathiasen et al. 2008). Indeed, high levels of infestation reduce host height and diameter growth (Mathiasen et al. 1990), suppress reproductive output and germination success (Sproule 1996), increase water stress, and reduce host vitality (Sala et al. 2001). Their negative effect can be especially important in forests if recruitment of new host individuals is slow, or during ecologically stressful conditions such as drought (Spurrier and Smith 2007). Given these positive and negative effects of mistletoes, research on mistletoe infestation prevalence at host population level in fragmented landscapes is needed to understand how land use change affects the prevalence and distribution of host–parasite interactions.

Here, we combined high-resolution airborne imaging spectroscopy + LiDAR and a ground-based survey to investigate three aspects of mistletoe–host interactions: (1) detection accuracy of mistletoes and their oak phorophytes; (2) hemiparasitism prevalence within host tree canopies depending on tree height; and (3) spatial variation in hemiparasitism across fragmented woodlands under the expectation that host canopies of isolated trees and along forest edges would be more susceptible to infestation due to increased light availability and seed rain.

Methods

Study area

The study was carried out at the Jasper Ridge Biological Preserve (JRBP) located in northern California, USA. The vegetation is primarily composed of Mediterranean-type communities including chaparral, wetlands, mixed evergreen forest, and oak woodland, covering a total area of 481 ha. Mean annual precipitation is ~600 mm, with the majority of it occurring between November and April. Forest edges are prominent throughout the preserve, resulting from a combination

of past deforestation and the presence of woodland–grassland mosaic ecotones (Bocek and Reese 1992). This landscape is characterized by the presence of small and large remaining woodland fragments, in addition to a large number of isolated oak trees, extensive edges between forest patches, and open areas.

Airborne data collection and data processing

In July 2013, when trees were fully leafed, the Carnegie Airborne Observatory (CAO) Airborne Taxonomic Mapping System (AToMS) acquired high-resolution data of JRBP using an integrated tool set consisting of a full-range imaging spectrometer (Visible and Shortwave Infrared imaging spectrometer; VSWIR) and waveform LiDAR scanner. The integrated AToMS processing stream is described in Asner et al. (2012) and briefly summarized here. The imaging spectrometer provides spectral radiance data in 5-nm increments from 380 to 2510 nm. The spectrometer was flown at 1000 m altitude above ground level, collecting VSWIR data at 1.0-m ground sampling distance (pixel size) throughout the study landscape. We created a digital terrain model (DTM) and a digital surface model (DSM) using the LiDAR data, which were used to precisely ortho-geolocate the VSWIR data and to remove shaded pixels (Asner et al. 2007).

The VSWIR data were radiometrically corrected from raw digital number values to radiance ($W \cdot sr^{-1} \cdot m^{-2}$) using a flat-field correction, radiometric calibration coefficients, and spectral calibration data collected in the laboratory. The radiance data were atmospherically corrected to apparent surface reflectance using the ACORN-5 model (Imspec, Glendale, California, USA) and a method to suppress illumination and view-angle artifacts (Colgan et al. 2012). Spectral data were convolved to 10 nm. We removed water absorption bands and bands near the instrument measurement boundaries, resulting in 148 bands of VSWIR data. As we were interested only in green leaves, and to avoid shaded areas, we further filtered for VSWIR pixels with a normalized difference vegetation index greater than 0.5, and mean near-infrared (850–1050 nm) reflectance greater than 20%. Using the LiDAR data, we calculated the top-of-canopy height (TCH; Means et al. 1999, Lefsky et al. 2002), which provides an estimate of the maximum vegetation height in each pixel (1 m of spatial resolution; Appendix S1: Fig. S1). We calculated different landscape structural metrics using the LiDAR TCH, as described in *Methods: Landscape structure classification*.

Merging field and CAO data

From March to April 2014, we collected ground data on 216 host trees, 121 of them infected by a total of 455 mistletoe plants. As field surveys were carried out in spring, trees were partially without leaves, facilitating mistletoe identification in the field. Our sampled trees were selected by an intensive search for infected trees and subsequently a random selection of uninfected trees. Both samples of trees, infected and uninfected, were spread throughout the study landscape. Although crown health conditions of each surveyed tree, such as diseases, insect infestation, and poor nutrition content, were not the focus of our study, we did not notice evident disease symptoms or insect infestations. In addition, our sampled trees were spread throughout the study landscape, which ensured that infected and uninfected trees in different environmental and ecological conditions were sampled.

Using a combination of a smartphone and Bluetooth-enabled GPS/GLONASS receiver (Garmin, Olathe, Kansas, USA), we manually delineated the limits of each surveyed tree crown in the field, and estimated a point location for each mistletoe. The field and VSWIR data were spatially linked. To guide the identification of the surveyed crowns and mistletoes on the image, we uploaded into the smartphone a composite image derived from the first three principal components of the VSWIR imagery (Appendix S1: Fig. S2). We measured the distance between mistletoes and the ground using a laser distance meter (Leica DISTRO; Leica, Wetzlar, Germany). Considering the position of the mistletoes on the canopy (top, middle, or bottom area) and the presence or absence of tree branches over them, we classified the mistletoes in tree groups: top, partially hidden, and hidden. In addition, mistletoe diameter was estimated by estimating the distance between its horizontal limits from the ground. The mistletoe position and size were grouped into classes (Table 1). These classes were used as a proxy to determine the effect of the mistletoe size and position within the crown on its detectability by the

TABLE 1. Description of the classes used to evaluate the binary support vector machine models to predict mistletoe (*Phoradendron leucarpum*) prevalence in oak trees (*Quercus lobata*, *Q. douglasii*, *Q. kellogii*).

Classes	Description
Host–hemiparasite	Separation of oak canopy and mistletoes (in one class) from other land cover classes (i.e. soil, water, non-host trees, etc.)
Size	Large (>1.5 m diameter) and small (<1.5 m diameter)
Presence	Presence of mistletoes
0	Absence of mistletoes
1	Large mistletoes, located at the top of the canopy
2	Small mistletoes, located at the top of the canopy
3	Large mistletoes, partially hidden by the canopy
4	Small mistletoes, partially hidden by the canopy
5	Large mistletoes, hidden by the canopy
6	Small mistletoes, hidden by the canopy

CAO (see *Methods: Host–hemiparasite mapping using support vector machine classification*).

We merged the CAO and field data to obtain three analytical variables. The first was the mean canopy height of infected and uninfected trees. This variable was calculated using the mean LiDAR TCH value from each infected and uninfected tree assessed. The second was the relative height (RH) of the mistletoes within the host canopy. RH is the distance from each mistletoe to the top of the canopy covering them. RH was calculated by subtracting the LiDAR TCH by the distance between the mistletoe and the ground (field data). The third variable was the mean reflectance value using VSWIR imagery. Mistletoe mean reflectance was obtained by selecting all VSWIR pixels within a 2 m radius buffer at the location of each surveyed mistletoe. Mean reflectance exclusively from infected trees was obtained by excluding VISWIR pixels of mistletoes located within polygons identified as infected host canopies. The mean reflectance of uninfected hosts was obtained by selecting VSWIR pixels from uninfected hosts. For these three classes (1 [mistletoes], 2 [infected hosts], 3 [uninfected hosts]), we calculated the mean reflectance value using the VSWIR data.

Host–hemiparasite mapping using support vector machine classification

Support vector machine (SVM) is a nonparametric classifier that separates classes into multidimensional space and efficiently processes large amounts of input data (Melgani and Bruzzone 2004). We used 146 spectral bands of VSWIR data (380–2510 nm) as input in binary SVM models to test the spectral separability between different classes such as presence/absence of the host or hemiparasite. Different classes (Table 1) were also compared for their spectral separability by using binary SVM models.

In our SVM classification framework, we first optimized the model parameters for the radial basis function kernel, such as the gamma and the cost. A large range of values (10^{-10} to 10^{10}) was used to select the best parameters. This procedure ensured the selection of the best parameters, considering trade-offs between model complexity, overfitting or underfitting, and number of training data (Ben-Hur and Weston 2009). Second, we randomly separated 70% of the data as a training set and 30% as a validation set. The training set was used to predict binary classes and the validation set was used to evaluate the model performance. This performance was calculated using the balanced accuracy (BAC) formula of Féret and Asner (2012):

$$\mathrm{BAC} = \frac{P(A)+P(B)}{2} \times 100$$

where BAC is the balanced accuracy of the SVM predictions to separate two classes, P(A) is the proportion of pixels correctly classified in class A (i.e., mistletoe leaves), and P(B) is the proportion of pixels correctly classified in class B (i.e., oak leaves). We repeated this procedure 100 times by random selection of the training and validation of data sets, and subsequently we calculated the mean and standard deviation (SD) of BAC.

Optimal SVM models (higher BAC) were used to automatically map host and hemiparasite throughout the studied landscape. First, we mapped the study area as two classes: (1) host–hemiparasite class (oaks and mistletoes as a single class) and (2) any other land cover class (i.e., soil, water, non-host trees, scrublands, etc.). As we obtained a high accuracy to separate these two classes (see *Results*), we used only the pixels from the host–hemiparasite class to perform subsequent mapping procedures. In a second step, the host–hemiparasite class was separated into two other classes: (1) presence and (2) absence of mistletoes. Finally, we used pixels identified as mistletoes to separate them into classes describing mistletoe size and its position in the host canopy (see definition of each class in Table 1). The classification accuracy for each mapping step was reported by the mean and standard deviation of the BAC.

The mistletoe prevalence, defined as the proportion of the host canopy surface infected by mistletoes, was obtained by comparing the number of pixels identified as mistletoes with the number of pixels identified as host canopy. We then evaluated the mistletoe prevalence in different landscape contexts (see *Methods: Landscape structure classification*).

Landscape structure classification

We separated the LiDAR TCH data into six classes (<5, 5.1–10.0, 10.1–15.0, 15.1–20.0, 20.1–25.0, and >25.1 m), as shown in Appendix S1: Fig. S1. These classes represent canopy height ranges where mistletoe infestation is likely to occur. For that purpose, we assessed the mistletoes' prevalence over the host trees located in each of these six TCH classes. In a second procedure for the landscape structure classification, we used the mean TCH within a 30 m radius surrounding each focal pixel as a variable correspondent to the canopy architecture. In a moving window approach, each focal pixel was reclassified using the mean TCH within the defined radius (30 m). Subsequently, this reclassified image was used to separate the whole study area into three classes: isolated (individual) trees, forest edge, and forest interior. These classes were defined as follows. Low mean value of TCH (<3 m) within a 30 m radius was classified as the isolated tree class. Intermediate ($3 \geq \mathrm{TCH} \geq 9$ m) and high (TCH > 9 m) mean values of TCH were classified as forest edge and interior, respectively. We assessed the separability among these three classes using a sensibility analysis, in which we tested different TCH threshold values to

separate the classes (see Appendix S1: Table S11 for detail). Finally, we overlaid this landscape classification (isolated trees, forest edge, and forest interior) with the host–parasite map and calculated the cover area of host and hemiparasite into the landscape classes, as indicative of infestation prevalence.

Results

Host and hemiparasite mapping

We mapped host–hemiparasite spatial distribution as a unique class and achieved a testing accuracy (BAC) of 96% (SD = 0.9%) in discriminating them from all other land cover classes: non-hosts trees, scrubs, herbs, soil, water, and buildings. When separating hemiparasites into different classes within oak canopies only, we obtained accuracy of 93% (SD = 1.46%) in discriminating large mistletoes at the top of the canopy and accuracy of over 80% for mistletoes partially hidden within the canopy (Fig. 1).

We had better SVM performance when classifying mistletoe presence and absence (86%, SD = 0.8%) than when separating mistletoes into large and small (55%, SD = 5.0%). Applying the best SVM models to map host and mistletoes through the biological preserve, we found that 11.8% of the overall vegetation cover corresponds to host trees and that ~8% of the canopy area is covered by mistletoes (Fig. 2).

VSWIR pixels dominated by oak and mistletoe showed different spectral curves (Fig. 3). The spectral separability between the host and hemiparasite leaves occurred across a broad spectral range (Fig. 3A), for example throughout the near-infrared (800–900 nm) as well as in the shortwave infrared (1200–2500 nm). These differences in spectral signature between oaks and mistletoes permitted us to map these plants with high accuracy, as described earlier. Surprisingly, oak leaves from infected and uninfected canopies also showed different spectral curves in the near-infrared wavelength range (Fig. 3B). We obtained a BAC of 75% (SD = 0.8) when comparing leaf spectral signature of infected and uninfected oak canopies.

Combined features of CAO, the high-resolution spectral data, and mistletoe traits (size and position within the host canopy) enabled the effective mapping of host and hemiparasite. Field data showed that mean mistletoe diameter was 1.5 m (SD = 0.7 m). In addition, mistletoes were often close to the upper edge of the tree crown, facilitating their detection with the high-resolution images (cf Appendix: Fig. S12). We found a large number of mistletoes (70%) with a RH value lower than 5.0 m (Fig. 4), and the mean RH of all mistletoes was 2.63 m (SD = 2.84 m).

Forest and landscape structure filtering of host–parasite interaction

The mean TCH of trees infected with mistletoes was 10.6 m (SD = 5.3 m). The mean TCH of uninfected trees was slightly lower (10.0 m; SD = 4.6 m), but not significantly so ($P > 0.05$). However, the highest TCH value for both tree categories differed for infested and uninfested trees (29.6 and 27.0 m, respectively). Separating the mean TCH of the host area among each landscape class, we found that isolated host trees were the shortest (TCH = 8.2 m; SD = 3.6 m), followed by those host trees at the forest edge (TCH = 9.5 m; SD = 3.8 m) and forest interior (TCH = 14.2 m; SD = 4.7 m). Host canopy surfaces

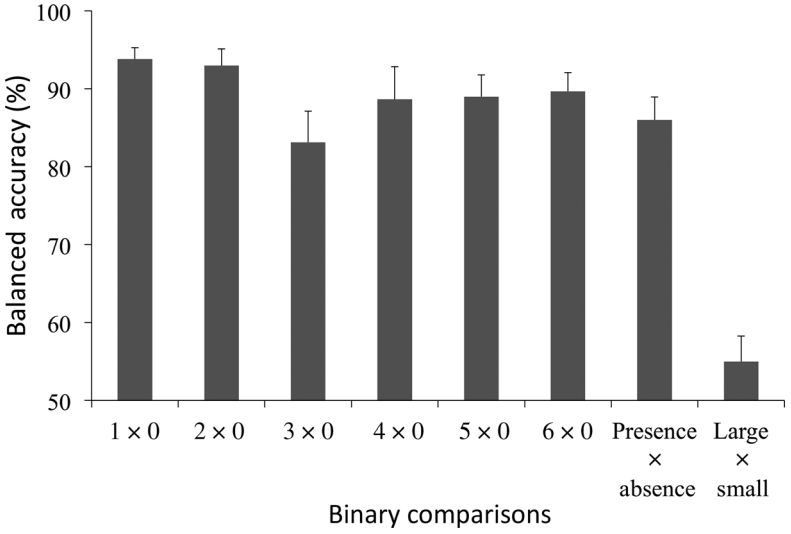

FIG. 1. Comparison of the mean balanced accuracy among binary classes. Error bars represent standard deviation. Classes being compared are described in Table 1.

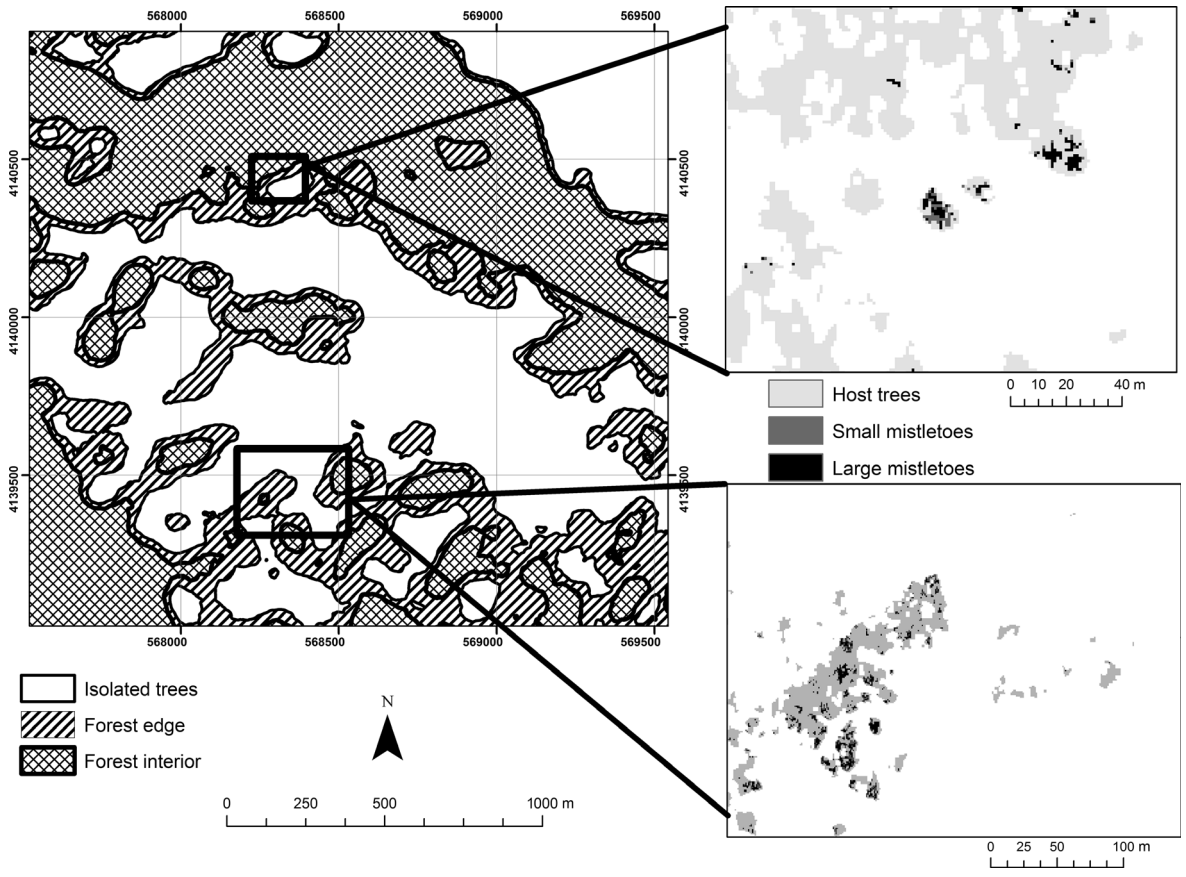

FIG. 2. Host–hemiparasite map (coordinates given in UTM) using high-resolution imaging spectroscopy and landscape classes (isolated trees, forest edge, forest interior).

with TCH ranging from 5 to 15 m represented ~80% of the study area (Fig. 5A). At this canopy height, mistletoes were more likely to be found than in all other host canopy height classes (Fig. 5B). There was an increase in the proportion of large mistletoes as TCH of host trees increased (Fig. 5B).

We tested a large range of criteria to classify the landscape into isolated trees, forest edge, and interior. Considering the classified landscapes, we found that the probability of the host being infested by hemiparasites increases following an ecological gradient of forest interior > forest edge > isolated trees. Although there was a larger host area infected by mistletoes in the forest edge compared with isolated trees or forest interior (Fig. 6A), isolated host trees showed higher infestation prevalence (Fig. 6B). A sensibility analysis supported our findings, even when we modified the criteria to classify the study landscape (Appendix: Table S11).

DISCUSSION

Using a combination of fieldwork and airborne imaging spectroscopy, we were able to map both host trees and hemiparasites with high accuracy, and to evaluate the mistletoe prevalence over oak trees located in different landscape contexts, including edge or core area of forest fragments. Several of our remote sensing SVM models for host and hemiparasite mapping showed high accuracy, with the most accurate being those detecting large mistletoes at the top of the canopy, relative to more hidden mistletoes. The good performance of the SVM classification may be associated with the subtle but consistent spectral differences between mistletoes and their hosts in the near-infrared and shortwave infrared spectral ranges. Differences among these spectral intervals suggest distinct leaf water content between species (Asner and Martin 2009, 2010), although pigments, leaf area and volume, and canopy architecture may also be important determinants (Curran 1989, Asner 1998). Moreover, Hollinger (1983) demonstrated important physiological differences between *Quercus lobada* and *Phoradendron villosum*, which may produce contrasting leaf chemical and spectral signatures (Doughty et al. 2011). This is an aspect that needs further study.

Classification accuracy for small and hidden mistletoes was also high. Light reflectance in the near-infrared

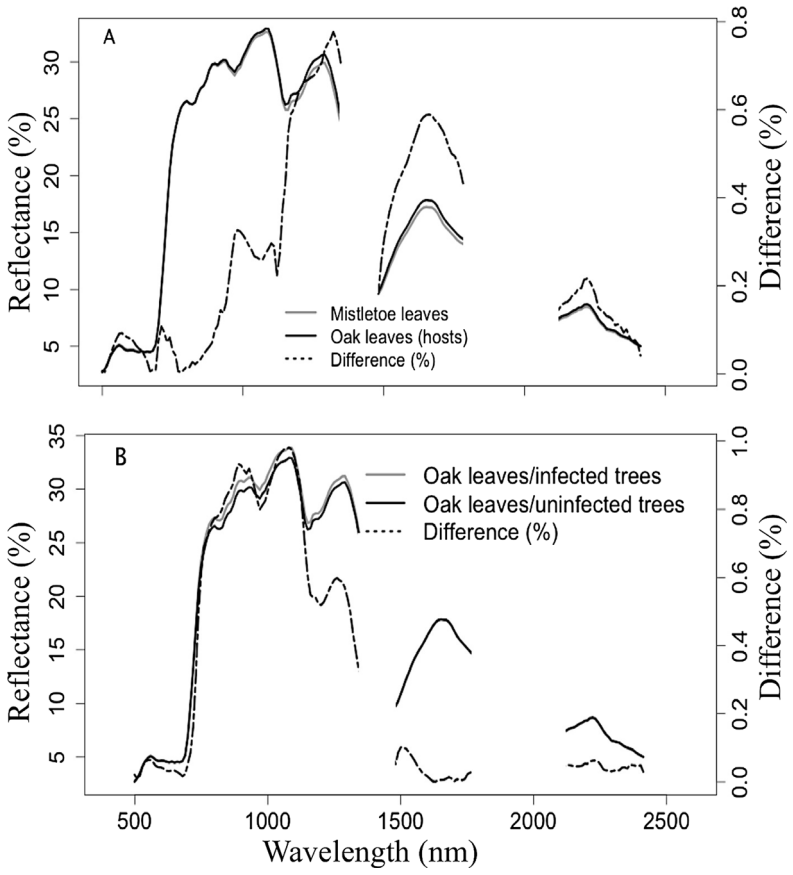

FIG. 3. Mean reflectance value (%) and differences between spectral curves (%) by wavelength (nm). (A) Spectral signature of oak trees (*Quercus lobata*, *Q. douglasii*, *Q. kellogii*) and mistletoes (*Phoradendron leucarpum*). (B) Spectral signature of infected and uninfected crowns of oak trees.

wavelength region likely derives from deeper portions within the canopy than reflectance from the visible wavelength (Ollinger 2011), which corroborates the importance of the near-infrared range in the detectability of mistletoes surrounded by oak leaves. As species identification using high-resolution imaging spectroscopy has been based on overall spectral signature of the canopy (Colgan et al. 2012, Baldeck et al. 2014), more attention should be given to the presence of different species under the target canopy.

Although spectral differences between host and hemiparasites were the primary focus of this study, we also found significant differences in canopy spectroscopy between oak leaves from infected and uninfected trees (BAC = 75%). Leaf chemical composition of infected and uninfected oaks was not evaluated in our study; however, recent studies have found consistent relationships between imaging spectroscopy and canopy chemical signatures (Townsend et al. 2003, Dahlin et al. 2013). Comparable spectral differences have been also found between pine trees infected and uninfected with mountain pine beetle, which are related to differences in total chlorophyll and water content among trees (Cheng et al. 2010). In addition, previous reports have indicated changes in chemical and physiological traits between infected

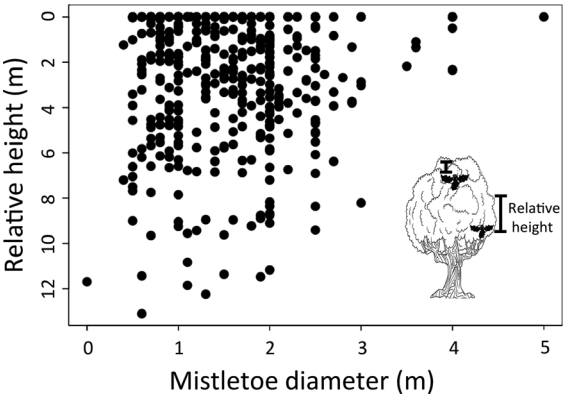

FIG. 4. Relationship between mistletoes' relative height (RH) and diameter using the field and LiDAR data. RH is the distance between the mistletoe height and the maximum canopy height above them. Mistletoe diameter greater than 3 m typically represents multiple, grouped mistletoes.

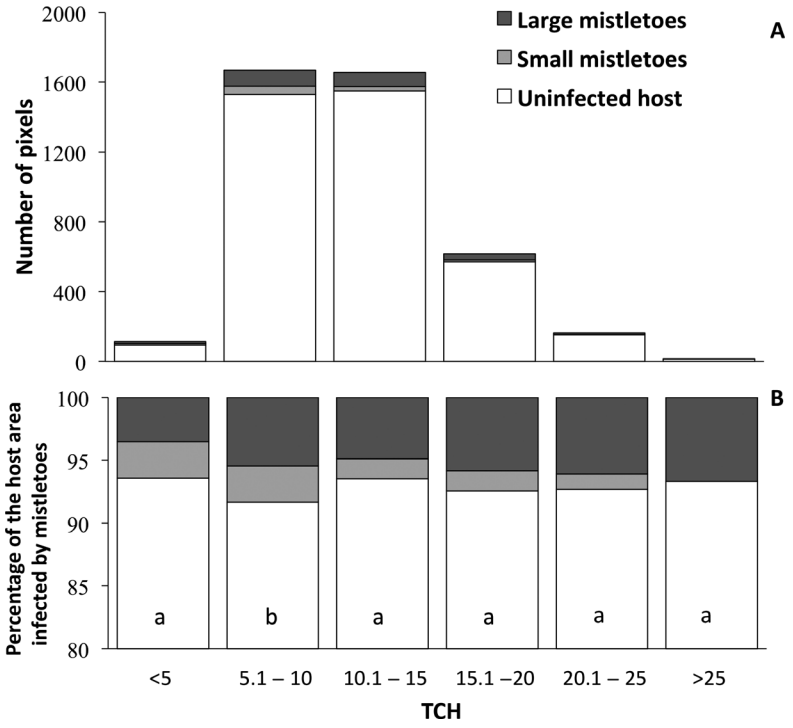

FIG. 5. Frequency and relative percentage of host and mistletoes at different top-of-canopy heights (TCH). (A) Frequency of pixels identified as host and hemiparasite-infected, by TCH. (B) Relative percentage of mistletoe cover classes: uninfected oak trees (*Q. lobata*, *Q. douglasii*, *Q. kellogii*) without mistletoes; large mistletoes >1.5 m diameter; small mistletoes <1.5 m diameter within each TCH class. Statistical differences ($P < 0.05$) between the percentage of infected and uninfected pixels across TCH classes are represented by different lowercase letters.

and uninfected hosts parasitized by mistletoes (Meinzer et al. 2004). These spectral differences in oak leaves from infected and uninfected trees suggest potential cascading effects of the fragmentation process on the overall leaf chemical traits of canopies. For example, due to changing landscape structure, parasitic prevalence may be enhanced on specific host locations and therefore nonrandomly affecting canopy chemistry.

We detected higher host area availability in forest edges than in forest interior or in isolated trees. The probability of the host being infested increased following an ecological gradient of forest interior < forest edge < isolated trees. These findings emerged when we analyzed the area of infested hosts in different landscape contexts weighted by the total host area available as habitat for mistletoes. Our results suggest that within-host mistletoe occurrence has a nonrandom spatial distribution mediated by landscape structure. These findings support the hypothesis that fragmentation affects patterns of host–parasite interactions (Magrach et al. 2014). Moreover, the results also indicate that forest management and conservation should consider how landscape configuration drives species interaction patterns. Although infestation happens at the individual level where selective forces operate, the landscape perspective gives us a large-scale assessment of the interaction patterns and indicates potential environmental drivers of the infestation mechanisms.

The exposure level of the canopy, as in open spaces, seems to be more important than canopy height for mistletoe infestation in our study area. Given that isolated or edge-located trees have their branches more exposed after fragmentation, these trees may enhance parasite prevalence due to a higher light availability within their canopy (Norton and Reid 1997). This is consistent with our finding that mistletoes were mainly located at the edge of canopy surfaces. Previous studies showed divergent results related to optimal canopy architecture for mistletoe infestation (Thomson and Mahall 1983, Ward 2005). Our study, based on LiDAR data, shows that infected and uninfected trees showed similar canopy architecture.

A striking result of this study is that isolated oak trees exhibited the highest infestation prevalence. Isolated hosts may be focal microsites for mistletoe seed dispersers, because these trees may operate as important stepping stones in the landscape (Gillies and St. Clair 2010). Moreover, dispersal of mistletoes depends on both specialist and generalist bird species as well as on contagious dispersal, where seeds are deposited very close to adult mistletoes (Watson 2012), resulting in an increase of parasites within seed-rain shadows (Reid

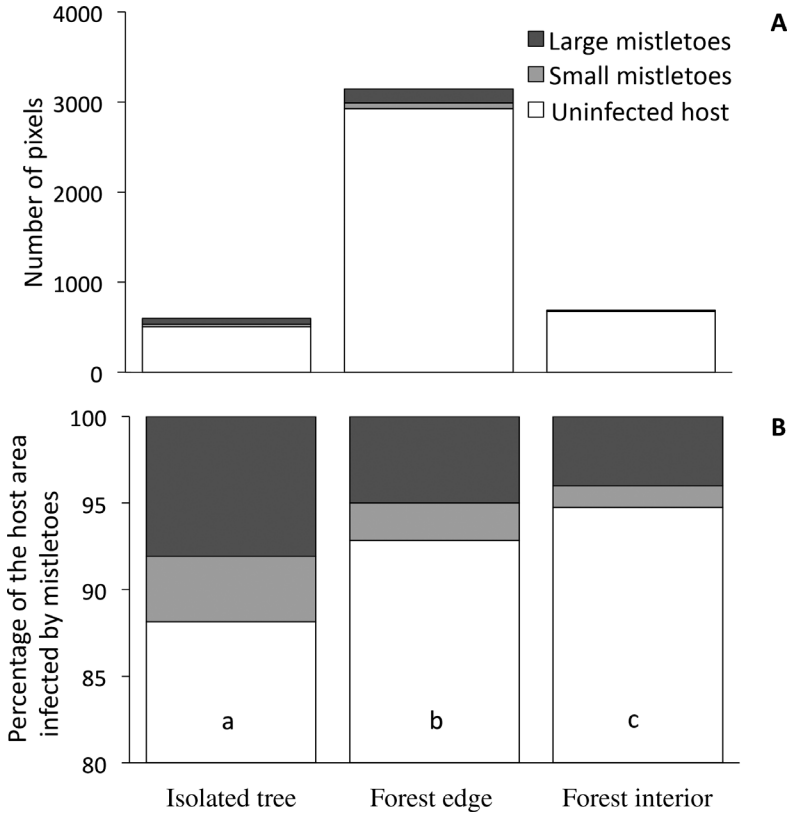

FIG. 6. Frequency and relative percentage of host and mistletoes at the landscape level. (A) Frequency of pixels from the host and hemiparasite cover classification considering position in the landscape (isolated trees, forest edge, and forest interior). (B) Relative percentage of mistletoe cover classes by landscape position: uninfected oak trees (*Q. lobata*, *Q. douglasii*, *Q. kellogii*) without mistletoes; large mistletoes >1.5 m diameter; small mistletoes <1.5 m diameter. Statistical differences ($P < 0.05$) between the percentage of infected and uninfected pixels across landscape positions are represented by different lowercase letters.

and Yan 2000). These dispersion patterns indicate the occurrence of a positive feedback in tree infestation due to spatial proximity and bird behavior.

Although fragmentation is already known as a potential driver of mistletoe proliferation (MacRaild et al. 2010, Magrach et al. 2013), our results, based on detailed quantitative information, indicate that host trees isolated in the landscape may have twice the chance of infestation by mistletoes than trees located at the core area of the forest fragments. The widespread infestation of trees located on the forest edge or isolated in the landscape has significant implications for conservation, especially considering that most woodland landscapes are fragmented and the global tendency for forested areas is a fragmentation rise (Costa et al. 2014, Laurance et al. 2014). Beyond landscape fragmentation, other natural or human-mediated disturbances are likely to enhance mistletoe infestation, including plant or animal invasive species and increased fire frequency and/or intensity (Parker et al. 2006).

Although mistletoes play a role as a food resource for some species of birds (fruits) and insects (foliage), high infestation loads may threaten the population of their hosts, with long-term cascading consequences. The effect of fragmentation on the interaction between mistletoes and their phorophytes has been previously explored by a few studies. For example, MacRaild et al. (2010) found that habitat fragmentation initially enhances mistletoe occurrence. Another study found that mistletoes have higher abundance in forest edges than in core areas of forest fragments (López de Buen et al. 2002). These pioneer studies assessed mistletoe prevalence and its variation in space; however, they did not analyze mistletoe prevalence weighted by total host availability. At a larger scale, information about mistletoe prevalence in the host population and how forest structure mediates parasite–host interaction is limited because of the difficulty to map infestation prevalence on landscapes.

From the landscape ecology perspective, our methodological approach could be applied to landscapes with different fragmentation levels to evaluate potential thresholds in the infestation prevalence. The use of the described methodological approach in structurally more complex and diverse forests may reveal additional

challenges in mapping hemiparasites or other vascular epiphytes. For instance, mistletoe host specificity and density may be lower in tropical forests compared with temperate forests (Norton and Carpenter 1998, Poltz and Zotz 2011), thereby requiring more effort to map host area available for the hemiparasites. Also, the complex vertical stratification of some tropical forests may represent a major challenge to map target hemiparasitic species. In the case of vascular epiphytes, lianas, and host trees, their leaves are often spectrally distinct and have significantly different leaf traits and pigment concentrations in tropical dry forests, while these differences are weaker in rainforests (Sánchez-Azofeifa et al. 2009). In sum, the potential for application of the methodologies described for this study is an aspect that warrants further research.

Integrating field, LiDAR, and spectroscopic measurements allowed us to assess hemiparasite–phorophyte interaction in a spatially explicit manner, adding a novel perspective to research programs on the effect of landscape structure on ecological systems. Furthermore, our study indicates that the use of advanced remote sensing technology can be of aid in monitoring plant infestation by hemiparasites in altered landscapes, an aspect of increasing significance in light of global environmental change.

Acknowledgments

The authors would like to thank P. Jordano for his valuable comments on the initial stage of this work. J. M. Barbosa was supported by CAPES Foundation, Ministry of Education, Brazil (grant number 11725/13-3). E. Sebastián-González was supported by the FAPESP Research Foundation, Brazil (grant number 2011/17968-2). Carnegie Airborne Observatory data acquisition, processing, and analysis were supported by a grant to G. P. Asner from the Gordon and Betty Moore Foundation. The Carnegie Airborne Observatory is made possible by the Avatar Alliance Foundation, Margaret A. Cargill Foundation, John D. and Catherine T. MacArthur Foundation, Grantham Foundation for the Protection of the Environment, W.M. Keck Foundation, Gordon and Betty Moore Foundation, Mary Anne Nyburg Baker and G. Leonard Baker Jr., and William R. Hearst III.

Literature Cited

Asner, G. P. 1998. Biophysical and biochemical sources of variability in canopy reflectance. Remote Sensing of Environment 64:134–153.

Asner, G. P., and R. E. Martin. 2009. Airborne spectranomics: mapping canopy chemical and taxonomic diversity in tropical forests. Frontiers in Ecology and the Environment 7:269–276.

Asner, G. P., and R. E. Martin. 2010. Canopy phylogenetic, chemical and spectral assembly in a lowland Amazonian forest. New Phytologist 189:999–1012.

Asner, G. P., D. E. Knapp, M. Jones, T. Kennedy- Bowdoin, R. E. Martin, C. B. Field, and J. Boardman. 2007. Carnegie airborne observatory: in-flight fusion of hyperspectral imaging and waveform light detection and ranging for three-dimensional studies of ecosystems. Journal of Applied Remote Sensing 1:013536.

Asner, G. P., D. E. Knapp, J. Boardman, R. O. Green, T. Kennedy-Bowdoin, M. Eastwood, R. E. Martin, C. Anderson, and C. B. Field. 2012. Carnegie Airborne Observatory-2: increasing science data dimensionality via high-fidelity multi-sensor fusion. Remote Sensing of Environment 124:454–465.

Baldeck, C. A., M. S. Colgan, J. B. Féret, S. R. Levick, R. E. Martin, and G. P. Asner. 2014. Landscape-scale variation in plant community composition of an African savanna from airborne species mapping. Ecological Applications 24:84–93.

Ben-Hur, A., and J. Weston. 2009. A user's guide to support vector machine. Pages 223–239 in J. M. Walker, editor. Methods in molecular biology. Humana Press, Totowa, New Jersey, USA.

Bennett, A. F., and D. A. Saunders. 2010. Habitat fragmentation and landscape change. Pages 88–106 in N. S. Sodhi, and P. R. Ehrlich, editors. Conservation biology for all. Oxford University Press, Oxford, UK.

Bocek, B., and E. Reese. 1992. Land use history of Jasper Ridge Biological Preserve. Jasper Ridge Research Report No. 8. Stanford University, Stanford, California, USA.

Cagnolo, L., G. Valladares, A. Salvo, M. Cabido, and M. Zak. 2008. Habitat fragmentation and species loss across three interacting trophic levels: effects of life-history and food-web traits. Conservation Biology 23:1167–1175.

Cheng, T., B. Rivard, G. A. Sánchez-Azofeifa, J. Feng, and M. Calvo-Polanco. 2010. Continuous wavelet analysis for the detection of green attack damage due to mountain pine beetle infestation. Remote Sensing of Environment 114:899–910.

Colgan, M. S., C. A. Baldeck, J. Féret, and G. P. Asner. 2012. Mapping savanna tree species at ecosystem scales using support vector machine classification and BRDF correction on airborne hyperspectral and LiDAR data. Remote Sensing 4:3462–3480.

Cooney, S. J. N., and D. M. Watson. 2005. Diamond firetails *Stagonopleura guttata* preferentially nest in mistletoe. Emu 105:317–322.

Cooney, S. J. N., D. M. Watson, and J. Young. 2006. Mistletoe as a nest site for Australian birds: a review. Emu 106:1–12.

Cooper, C. B., and J. R. Walters. 2002. Independent effects of woodland loss and fragmentation on Brown Treecreeper distribution. Biological Conservation 105:1–10.

Costa, A., M. Madeira, and T. Plieninger. 2014. Cork oak woodlands patchiness: a signature of imminent deforestation? Applied Geography 54:18–26.

Curran, P. J. 1989. Remote sensing of foliar chemistry. Remote Sensing of Environment 30:271–278.

Dahlin, K. M., G. P. Asner, and C. B. Field. 2013. Environmental and community controls on plant canopy chemistry in a Mediterranean-type ecosystem. Proceedings of the National Academy of Sciences USA 110:6895–6900.

Debinski, D. M., and R. D. Holt. 2000. A survey and overview of habitat fragmentation experiments. Conservation Biology 14:342–355.

Doughty, C. E., G. P. Asner, and R. E. Martin. 2011. Predicting tropical plant physiology from leaf and canopy spectroscopy. Oecologia 165:289–299.

Echeverria, C., D. Coomes, J. Salas, J. M. Rey-Benayas, A. Lara, and A. Newton. 2006. Rapid deforestation and fragmentation of Chilean temperate forests. Biological Conservation 130:481–494.

Fahrig, L. 2003. Effects of habitat fragmentation on biodiversity. Annual Review of Ecology, Evolution, and Systematics 34:487–515.

Fáveri, S. B., H. L. Vasconcelos, and R. Dirzo. 2008. Effects of Amazonian forest fragmentation on the interaction between plants, insect herbivores, and their natural enemies. Journal of Tropical Ecology 24:57–64.

Féret, J. B., and G. P. Asner. 2012. Tree species discrimination in tropical forests using airborne 448 imaging spectroscopy. IEEE Transactions on Geosciences and Remote Sensing 51:73–84.

Fletcher, R. J. Jr, L. Ries, J. Battin, and A. D. Chalfoun. 2007. The role of habitat area and edge in fragmented landscapes: definitively distinct or inevitably intertwined? Canadian Journal of Zoology 85:1017–1030.

Gillies, C. S., and C. C. St. Clair. 2010. Functional responses in habitat selection by tropical birds moving through fragmented forest. Journal of Applied Ecology 47:182–190.

Hollinger, D. Y. 1983. Photosynthesis and water relations of the mistletoe, *Phoradendron villosum*, and its host, the California valley oak, *Quercus lobata*. Oecologia 60:396–400.

Joly, C. A., J. P. Metzger, and M. Tabarelli. 2014. Experiences from the Brazilian Atlantic Forest: ecological findings and conservation initiatives. New Phytologist 204:459–473.

Laurance, W. F., et al. 2011. The fate of Amazonian forest fragments: a 32-year investigation. Biological Conservation 144:56–63.

Laurance, W. F., J. Sayer, and K. G. Cassman. 2014. Agricultural expansion and its impacts on tropical nature. Trends in Ecology & Evolution 29:107–116.

Lefsky, M. A., W. B. Cohen, G. G. Parker, and D. J. Harding. 2002. Lidar remote sensing for ecosystem studies. BioScience 52:19–30.

López de Buen, L., J. F. Ornelas, and J. G. Gárcia-Franco. 2002. Mistletoe infection of trees located at fragmented forest edge in the could forests of central Veracruz, Mexico. Forest Ecology and Management 164:293–302.

MacRaild, L. M., J. Q. Radford, and A. F. Bennett. 2010. Non-linear effects of landscape properties on mistletoe parasitism in fragmented agricultural landscapes. Landscape Ecology 25:395–406.

Magrach, A., L. Santamaría, and A. R. Larrinaga. 2013. Forest edges show contrasting effects on an austral mistletoe due to differences in pollination and seed dispersal. Journal of Ecology 101:713–721.

Magrach, A., W. F. Laurance, A. R. Larrinaga, and L. Santamaria. 2014. Meta-analysis of the effects of forest fragmentation on interspecific interactions. Conservation Biology 28:1342–1348.

Mathiasen, R. L., F. G. Hawksworth, and C. B. Edminster. 1990. Effects of dwarf mistletoe on growth and mortality of Douglas fir in the Southwest. Great Basin Naturalist 50:173–179.

Mathiasen, R. L., D. Nickrent, D. C. Shaw, and D. M. Watson. 2008. Mistletoes: pathology, systematics, ecology and management. American Phytopathological Society 92:988–1006.

Means, J. E., S. A. Acker, D. J. Harding, J. B. Blair, M. A. Lefsky, W. B. Cohen, M. E. Harmon, and W. A. McKee. 1999. Use of large-footprint scanning airborne lidar to estimate forest stand characteristics in the western Cascades of Oregon. Remote Sensing of Environment 67:298–308.

Meinzer, F. C., D. R. Woodruff, and D. C. Shaw. 2004. Integrated responses of hydraulic architecture, water and carbon relations of western hemlock to dwarf mistletoe infection. Plant, Cell and Environment 27:937–946.

Melgani, F., and L. Bruzzone. 2004. Classification of hyperspectral remote sensing images with support vector machines. IEEE Transactions on Geoscience and Remote Sensing 42:1778–1790.

Norton, D. A., and M. A. Carpenter. 1998. Mistletoes as parasites: host specificity and speciation. Trends in Ecology and Evolution 13:101–105.

Norton, D. A., and N. Reid. 1997. Lessons in ecosystem management from management of threatened and pest loranthaceous mistletoes in New Zealand and Australia. Conservation Biology 11:759–769.

Ollinger, S. V. 2011. Sources of variability in canopy reflectance and the convergent properties of plants. New Phytologist 189:375–394.

Parker, T. J., K. M. Clancy, and R. L. Mathiasen. 2006. Interactions among fire, insects and pathogens in coniferous forests of the interior western United States and Canada. Agricultural and Forest Entomology 8:167–189.

Poltz, K., and G. Zotz. 2011. Vascular epiphytes on isolated pasture trees along a rainfall gradient in the lowlands of Panama. Biotropica 43:165–172.

Reid, N., and Z. Yan. 2000. Mistletoes and other phanerogams parasitic on eucalypts. Pages 353–384 in P. J. Keane, G. A. Kile, F. D. Podger, and B. N. Brown, editors. Diseases and pathogens of eucalypts. CSIRO Publishing, Collingwood, Australia.

Reid, N., Z. Yan, and J. Fittler. 1994. Impact of mistletoes (*Ayema miquelii*) on host (*Eucalyptus blakelyi* and *Eucalyptus melliodora*) survival and growth in temperate Australia. Forest Ecology and Management 70:55–65.

Rodríguez-Cabal, M. A., M. A. Aizen, and A. Novaro. 2007. Habitat fragmentation disrupts a plant–disperser mutualism in the temperate forest of South America. Biological Conservation 139:195–202.

Ruiz-Guerra, B., R. Guevara, N. Mariano, and R. Dirzo. 2010. Insect herbivory declines with forest fragmentation and covaries with plant regeneration mode: evidence from a Mexican tropical rain forest. Oikos 119:317–325.

Sala, O., et al. 2000. Global biodiversity scenarios for the year 2100. Science 287:1770–1774.

Sala, A., E. V. Carrey, and R. M. Callaway. 2001. Dwarf mistletoe affects whole-tree water relations of Douglas fir and western larch primarily through changes in leaf to sapwood ratios. Oecologia 126:42–52.

Sánchez-Azofeifa, G. A., K. Castro, S. J. Wright, J. Gamon, M. Kalacska, B. Rivard, S. A. Schnitzer, and J. L. Feng. 2009. Differences in leaf traits, leaf internal structure, and spectral reflectance between two communities of lianas and trees: implications for remote sensing in tropical environments. Remote Sensing of Environment 113:2076–2088.

Sproule, A. 1996. Impact of dwarf mistletoe on some aspects of the reproductive biology of jack pine. Forestry Chronicle 72:303–306.

Spurrier, S., and K. G. Smith. 2007. Desert mistletoe (*Phoradendron californicum*) infestation correlates with blue palo verde (*Cercidium floridum*) mortality during a severe drought in the Mojave Desert. Journal of Arid Environments 69:189–197.

Terborgh, J., et al. 2001. Ecological meltdown in predator-free forest fragments. Science 294:1923–1926.

Thomson, V. E., and B. E. Mahall. 1983. Host specificity by a mistletoe, *Phoradendron villosum* (Nutt.) Nutt. subsp. v*illosum*, on three oak species in California. Botanical Gazette 144:124–131.

Townsend, P. A., J. R. Foster, R. A. Chastain, and W. S. Currie. 2003. Application of imaging spectroscopy to mapping canopy nitrogen in the forests of the central Appalachian Mountains using Hyperion and AVIRIS. IEEE Transactions on Geoscience and Remote Sensing 41:1347.

Underwood, E. C., J. H. Viers, K. R. Klausmeyer, R. L. Cox, and M. R. Shaw. 2009. Threats and biodiversity in

the mediterranean biome. Diversity and Distributions 15:188–197.

Villard, M. A., and J. P. Metzger. 2014. Review: Beyond the fragmentation debate: a conceptual model to predict when habitat configuration really matters. Journal of Applied Ecology 51:309–318.

Ward, M. J. 2005. Patterns of box mistletoe *Amyema miquelii* infection and pink gum *Eucalyptus fasciculosa* condition in the Mount Lofty Ranges, South Australia. Forest Ecology and Management 213:1–14.

Watson, D. M. 2001. Mistletoe: a keystone resource in forests and woodlands worldwide. Annual Review of Ecology and Systematics 32:219–249.

Watson, D. M. 2002. Effects of mistletoe on diversity: a case-study from southern New South Wales. Emu 102:275–281.

Watson, D. M. 2012. The relative contribution of specialists and generalists to mistletoe dispersal: insights from a Neotropical forest. Biotropica 45:195–202.

Willson, M., T. I. De Santo, C. Sabag, and J. J. Armesto. 1994. Avian communities of fragmented south-temperate rainforests in Chile. Conservation Biology 8:508–520.

Wulder, M. A., C. C. Dymond, J. C. White, D. G. Leckie, and A. L. Carroll. 2006. Surveying mountain pine beetle damage of forests: a review of remote sensing opportunities. Forest Ecology and Management 221:27–41.

Supporting Information

Additional supporting information may be found in the online version of this article at http://onlinelibrary.wiley.com/doi/10.1890/14.2429.1/suppinfo